International Journal of Pressure Vessels and Piping 131 (2015) 45–51

Contents lists available at ScienceDirect

International Journal of Pressure Vessels and Piping

journal homepage: www.elsevier.com/locate/ijpvp

Elastic-plastic failure assessment of cold worked stainless steel pipes

Masayuki Kamaya*

Institute of Nuclear Safety System, Inc., 64 Sata, Mihama-cho, Mikata-gun, Fukui 919-1205, Japan

ARTICLE INFO

Article history:
Received 17 April 2015
Accepted 20 April 2015
Available online 29 April 2015

Keywords:
Cold working
Stainless steel
Two-parameter method
J-integral
Fracture toughness
Stress–strain curve

ABSTRACT

The change in fracture strength due to cold working was investigated for cracked stainless steel pipes. The cold working was introduced into Type 316 stainless steel plates. Then, material properties were identified in order to make elastic–plastic fracture assessments for a pipe with a circumferential crack under bending load. The two-parameter method was employed for deriving fracture strength considering the change in the flow stress (yield and ultimate strengths), fracture toughness and stress–strain curve caused by the cold working. It was found that the fracture strength was not reduced even if 40% cold working was introduced, while the failure mode was altered from the plastic collapse mode to the elastic–plastic failure mode. Although cold working decreased the fracture toughness, the change in the stress–strain curve reduced the driving force for fracture (J-integral) and increased the fracture strength. It was shown that the failure assessment curve of cold worked material can be derived using the yield and ultimate strengths of the material that is free of cold working.

1. Introduction

Nuclear power plant components may be hardened by a large external load caused by accidental events, earthquakes, welding and so on. Neutron irradiation and thermal embrittlement also bring about material hardening. Since the hardening increases the yield and ultimate strengths, load carrying capacity of the components is increased by the hardening. For austenitic stainless steel, even if cracks are present in the components, the plastic collapse failure mode is assumed in fracture strength assessments according to the fitness-for-service codes [1,2]. In the assessment, the limit load is used as the fracture strength and it is increased by the hardening due to increases in the flow stress, which is the average of the yield and ultimate strengths [1,2]. On the other hand, the hardening (cold working) reduces the ductility accompanying the reduction in the fracture toughness. It has been shown that the cold working reduced the fracture toughness of carbon steel [3], low-alloy steel [4–6], aluminum alloy [7,8] and stainless steel [9,10], although the fracture toughness was increased by a relatively small amount of cold working of less than 5% in some experiments [5,11]. This may alter the failure mode from the plastic collapse mode to the unsteady ductile crack growth (hereafter, elastic–plastic failure mode) and reduce the fracture strength.

The fracture strength for the elastic–plastic failure can be assessed using fracture toughness (J_{IC} or J-R curve) as the material resistance and the J-integral as the driving force for fracture. Since the J-integral is obtained by elastic–plastic finite element analysis (FEA) using the stress–strain curve, the change in the stress–strain curve due to the hardening affects the failure assessment. Therefore, in order to assess the change in fracture strength of the cracked stainless steel components due to the hardening, the change in the material strength, fracture toughness and stress–strain curve brought about by the hardening have to be taken into account.

In this study, the change in fracture strength due to hardening was investigated for cracked stainless steel pipes. The hardening was simulated by cold working introduced by a rolling process. First, the change in material properties of the cold worked stainless steel was determined for various degrees of cold working. Then, elastic–plastic fracture assessments were conducted for a pipe with a circumferential crack under bending load. The characteristic feature of the change in fracture strength due to cold working was discussed. Finally, the assessment procedure for the cold worked stainless steel was shown.

2. Material properties

2.1. Tensile and fracture toughness tests

Type 316 stainless steel plates were used; the alloying constituents were (mass %): C, 0.06; Si, 0.84; Mn, 0.84; P, 0.028; S, 0.001;

* Tel.: +81 50 7105 0096; fax: +81 770 372009.
E-mail address: kamaya@inss.co.jp.

http://dx.doi.org/10.1016/j.ijpvp.2015.04.008
0308-0161/

Ni, 10.10; Cr, 16.16, Mo, 2.14 and balance Fe. The plates were subjected to a rolling process at room temperature in order to introduce the cold working. The original thickness of 45 mm was reduced by 5%, 10%, 20% and 40%. The materials were then respectively referred to as CW5, CW10, CW20 and CW40, while CW0 denoted the material free of cold working. The tensile properties and *J-R* curves for these materials have been obtained in a previous study [11].

Tensile tests were conducted using cylindrical specimens of 6 mm diameter machined along the rolling direction. Table 1 summarizes the tensile properties obtained. Fig. 1 shows the change in the yield (0.2% proof) and ultimate strengths with the degree of cold working. The material strengths increased monotonically with the degree of cold working.

Fracture toughness tests were conducted using standard type compact tension specimens with side grooves. The thickness of the specimens was 25 mm except for CW40. The CW40 rolled plate was not thick enough, and the thickness of the CW40 specimen had to be reduced to 20 mm, but this still satisfied the specification of the ASTM standard [12]. The direction normal to the crack plane was the same as the rolling direction (L-T direction). The tests were conducted according to the ASTM standard E1820-08 [12] in ambient air at room temperature, which was kept at 296 K. The crack growth size was identified by the compliance method. Fig. 2 shows the *J-R* curves obtained by the tests. The curve for CW0 could not be obtained. The fracture toughness was decreased as the degree of cold working was increased. The *J-R* curves were approximated by:

$$J = C_1(\Delta a)^{C_2} \quad (1)$$

where units for J and Δa are [kJ/m^2] and [mm], respectively. C_1 and C_2 are the material constants and they were obtained by the root mean square method using data of more than the 0.2 mm offset line so as to take the J-integral value that was more than J_Q. The identified parameters and the fracture toughens are shown in Table 1. J_Q values were obtained for CW20 and CW40. No J_{IC} or J_Q values could be obtained for CW5 and CW10 in addition to CW0.

2.2. Stress–strain curves

In order to conduct elastic–plastic FEA for the J-integral calculation, the stress–strain curves were identified. Fig. 3 shows the relationship between true stress and true plastic strain obtained by the tensile tests. The nominal stress–strain relation was transferred to the true stress–strain relation assuming that the specimens elongated uniformly even after necking had occurred. The test speed was changed from 10 MPa/s in stress to 0.5%/s in strain when nominal strain reached 2%. The change in the test speeds resulted in the discontinuity in the stress–strain curves at about 2% strain.

The stress–strain curve for CW40 exhibited only small uniform elongation and it was difficult to use for the FEA. Even if necking occurred during the tensile tests, the material continued hardening until the specimen failed. In order to simulate a large deformation in the vicinity of the crack tip for deriving the J-integral, it is necessary to obtain the true stress–strain curve after necking. Then, the curve after necking was obtained by the specified procedure using the digital image correlation (DIC) technique, which is referred to as the IFD (Iteration FEA procedure based on DIC measurement) method [13]. The strain and stress at the root of the necking portion were identified by strain measurement using the DIC technique and by iteration of the FEA, respectively. As shown in Fig. 3, the work hardening behavior of CW40 after necking could be successfully identified by the IFD method.

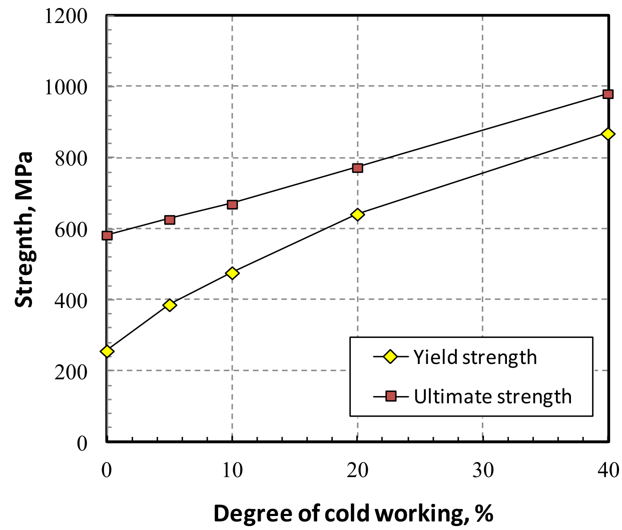

Fig. 1. Change in yield and ultimate strengths with degree of cold working.

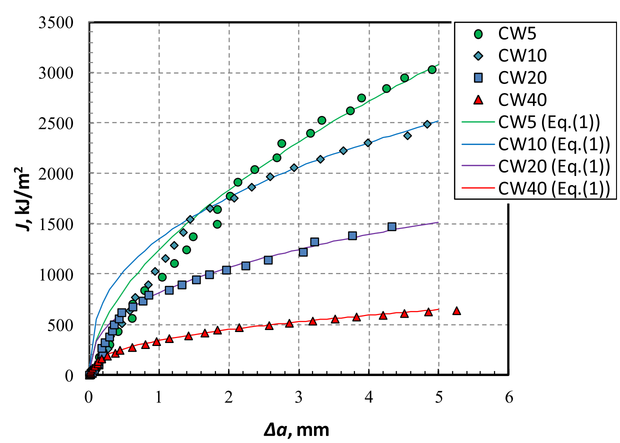

Fig. 2. *J-R* curves obtained for cold worked stainless steel and regression curves approximated by Eq. (1).

Table 1
Summary of tensile properties, constants for the *J-R* and stress–strain curves of cold worked (CW) Type 316 stainless steel.

CW (%)	Yield strength (MPa)	Tensile strength (MPa)	Elongation (%)	Reduction in area (%)	Young's modulus (GPa)	Stress–strain curve		Fracture toughness		
						A	ε_0	J_Q (KJ/m^2)	C_1	C_2
0	258	584	60.3	83.0	205	1313	0.0402	–	–	–
5	388	628	52.3	81.2	197	1350	0.0895	–	1239	0.566
10	478	671	45.3	80.0	193	1388	0.131	–	1344	0.389
20	643	774	33.0	78.3	191	1510	0.205	726	812	0.388
40	870	982	19.7	73.6	183	1438	0.469	207	338	0.401